Available online at www.sciencedirect.com
SCIENCE DIRECT®
Journal of Chromatography A, 1064 (2005) 75–84
JOURNAL OF CHROMATOGRAPHY A
www.elsevier.com/locate/chroma

Immobilised artificial membrane chromatography coupled with molecular probing
Mimetic system for studying lipid–calcium interactions in nutritional mixtures

Vanessa Hernando[a,b,c,*], André Rieutord[a,b], Robert Pansu[c], Françoise Brion[b], Patrice Prognon[a]

[a] *Groupe de Chimie Analytique de Paris Sud, EA 3343, Laboratoire de Chimie Analytique, Faculté de Pharmacie, 5 Rue Jean Baptiste Clément, 92296 Châtenay-Malabry Cedex, France*
[b] *Service de Pharmacie et Laboratoire de Toxico-Pharmacologie, Hôpital Robert Debré (AP-HP), 48 Boulevard Sérurier, 75935 Paris Cedex 19, France*
[c] *Laboratoire de Photophysique et Photochimie Macromoléculaires et Supramoléculaires (PPSM), CNRS UMR 8531, Ecole Normale Supérieure de Cachan, 61 Avenue du Président Wilson, 94235 Cachan Cedex, France*

Received 4 June 2004; received in revised form 30 November 2004; accepted 2 December 2004
Available online 29 December 2004

Abstract

Immobilised artificial membrane (IAM) chromatography was utilised to study the interactions of usual membrane probes with grafted phosphatidylcholine silica support, in relation to the presence of calcium ions introduced in the mobile phase as they are present in nutritional mixtures. IAM acts as a mimetic membrane of lipid emulsion globules, a major component of nutritional mixtures. The tested probes were 1,6-diphenyl-1,3,5-hexatriene (DPH), 9-diethylamino-5H-benzo[α]phenoxazine-5-one or nile red (NR) and 2-(*p*-toluidinyl)naphtalene-6-sulfonate (TNS). For each probe, partition coefficients and thermodynamic parameters of transfer from the mobile phase to the IAM stationary phase have been measured. Our results suggested that the interactions of neutral probes (i.e. DPH and NR) with phosphatidylcholine are driven by hydrophobic forces. Addition of calcium chloride to the mobile phase slightly decreased the retention of these neutral probes and dramatically increased that of anionic TNS. Moreover, an enthalpy–entropy compensation study revealed that the mechanism of interaction between TNS and IAM is independent of the calcium concentration. Results argued for the existence of electrostatic repulsion forces exerted by IAM phase towards anionic TNS. Addition of calcium ions into the mobile phase led to the establishment of an ionic double layer at the zwitterionic stationary phase surface weakening the electrostatic barrier and increasing TNS retention. Consequently, it was demonstrated that IAM appears as a suitable model to get a better insight on the lipid–calcium interactions taking place in nutritional mixtures.

Keywords: Immobilised artificial membranes; Phosphatidylcholine; Membrane probes; Thermodynamic parameters; Lipid–calcium interactions; Total parenteral nutrition

1. Introduction

Total parenteral nutrition (TPN) consists of formulations of glucose, amino acids and lipid emulsion supplemented by electrolytes, vitamins and trace elements. These mixtures intravenously administered provide complete nutritional support for patients. The destabilisation of the lipid emulsion

* Corresponding author. Present address: Laboratoire de Contrôles Physico-Chimiques et Biologiques (LCPCB), AGEPS, 7 Rue du fer à moulin, BP 09, 75221 Paris Cedex 05, France. Tel.: +33 1 46 69 14 82; fax: +33 1 46 69 14 92.
E-mail address: vanessa.hernando@eps.ap-hop-paris.fr (V. Hernando).

0021-9673/$ – see front matter © 2004 Elsevier B.V. All rights reserved.
doi:10.1016/j.chroma.2004.12.012

in the presence of electrolytes is a major problem [1]. Recently, it was shown that fluorescent probes appeared to be a useful analytical tool for the direct spectroscopic investigation of lipid–calcium ions interactions in TPN mixtures [2]. However, experimental difficulties were pointed out due to light scattering in turbid samples like TPN mixtures. Hence, the assessment of quantitative data, as the partition coefficients of the probes in the emulsion and the binding constant of calcium ions to the lipid droplets, was hazardous. We thought that immobilised artificial membrane (IAM) chromatography could be helpful to overcome these experimental difficulties. In fact, we can admit that there is a similarity between the interface of lipid droplets contained in TPN mixtures and the IAM stationary phase structures. Indeed, lipid droplets consist of a core of triglycerides surrounded by a monolayer of egg phospholipids [3]; phosphatidylcholine being the major component (80% (m/m)) of the latter. Phosphatidylethanolamine, phosphatidylglycerol, phosphatidic acid, phosphatidylinositol and phosphatidylserine are minor components. Although they are present in small amounts relative to phosphatidylcholine, some of them have a critical function in the emulsion stability by conferring negative surface potential on lipid droplets [1,4]. On the other hand, an immobilised artificial membrane appears as an in vitro chromatographic model of biological membranes in which synthetic phospholipid analogues are covalently linked as a monolayer to silica particles to form a stationary phase [5]. In particular, IAM.PC.DD2 material consists of diacyl double chain ester phosphatidylcholine ligands surface-bonded to an aminopropylsiloxane-bonded silica substrate and is endcapped by mixed propionic and decanoic alkylamide groups [6]. A typical IAM.PC.DD2 structure is presented in Fig. 1. IAM stationary phase offers polar head groups of phosphatidylcholine as the first site of contact with the solute and is therefore a more realistic model of biomembranes than octadecyl silica (ODS) reversed-phase chromatography columns. IAM is supposed to involve the same hydrophobic, ion-pairing, Van der Waals and hydrogen-bonding interactions exhibited by analytes in contact of biological membranes [5]. The grafted lipids of IAM also exhibit interfacial motional properties similar to those of the mobile lipids in fluid liposomes, as revealed by ^{31}P-NMR studies [7]. Therefore, retention on the IAM column possesses some similarities to biomembrane adsorption processes, allowing suitable correlation models to be developed for the estimation of certain biopartioning properties [6,8–11]. IAM chromatography had pharmacological [12,13] or pharmacokinetic applications as well [7,8,14,15]. It also allowed to mimic membrane interactions with peptides [16], ions [17] and bile salts [18]. In the same way, we propose to use IAM chromatography as a model of lipid droplets contained in TPN mixtures in order to dynamically study the lipid–calcium interactions using the variation of retention of some well-known molecular membrane probes.

The first objective of this study was to characterise the interaction of membrane probes with phosphatidylcholine monolayer in terms of partition coefficients and thermodynamic parameters of transfer from the mobile phase to the IAM stationary phase. The second objective was to study the effects of calcium ions on probes retention and, as a result, the lipid–calcium interactions using the extended Wyman relations [19,20] and an enthalpy–entropy compensation study [21]. Finally, whole IAM chromatographic results will be discussed in relation to the lipid–calcium interactions taking place in TPN mixtures.

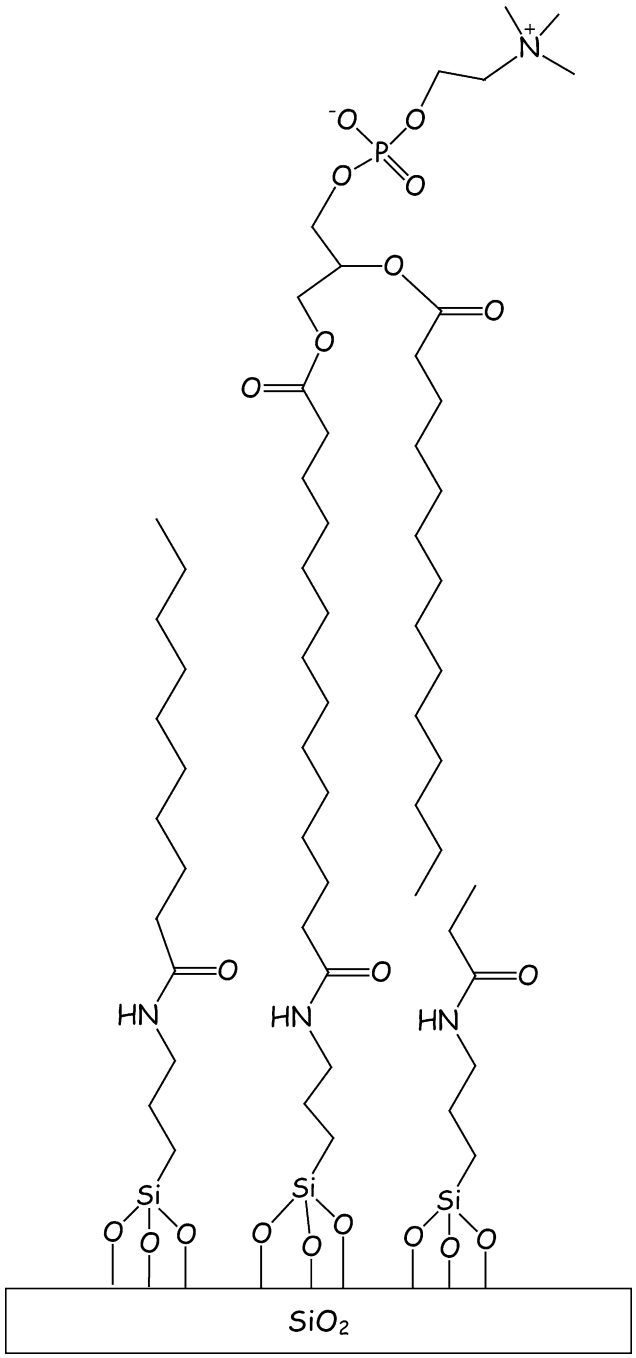

Fig. 1. Schematic structure of IAM.PC.DD2 stationary phase.

2. Theoretical

2.1. Determination of the probes partition coefficients

The isocratic retention times of the probe (t_r) are used to calculate the capacity factors k_{IAM} using the following equation:

$$k_{IAM} = \frac{t_r - t_0}{t_0} \quad (1)$$

where t_0 is the dwell time. A linear relationship exists between $\ln k_{IAM}$ and the organic volume fraction φ_{ACN}, according to:

$$\ln k_{IAM} = \ln k_W - a\varphi_{ACN} \quad (2)$$

where a is a constant and k_W the capacity factor in the absence of organic solvent. Hence, $\ln k_W$ can be determined by linear regression analysis by varying the organic volume fraction [22]. The capacity factor k_W is proportional to the equilibrium partition coefficient K_W of the probe between the phosphatidylcholine stationary phase and the aqueous phase according to:

$$k_W = \Phi K_W = \frac{V_{IAM}}{V_M}\frac{C_{IAM}}{C_W} \quad (3)$$

where Φ is the phase ratio of the column, with V_M volume of the mobile phase and V_{IAM} volume of the stationary phase. C_{IAM} and C_W are the concentrations of the solute in the stationary and in the aqueous phases, respectively. The volume of the stationary phase is known for the IAM column used in our case [23].

2.2. Thermodynamic parameters of the probe-stationary phase interactions

The Gibbs free energy, ΔG°, of solute transfer from the mobile phase to the stationary phase is related to K_{IAM}, the equilibrium distribution constant between the stationary and mobile phases, as follows:

$$\Delta G^\circ = -RT \ln K_{IAM} \quad (4)$$

where T is the absolute temperature in Kelvin and R the gas law constant.

ΔG° is also related to ΔH° and ΔS°, the standard enthalpy and entropy of transfer of the probes from the mobile phase to the stationary phase respectively:

$$\Delta G^\circ = \Delta H^\circ - T\Delta S^\circ \quad (5)$$

ΔH° and ΔS° can be calculated using the following thermodynamic relationship, derived from Eqs. (3)–(5):

$$\ln k_{IAM} = -\frac{\Delta H^\circ}{RT} + \frac{\Delta S^\circ}{R} + \ln \Phi \quad (6)$$

A linear plot of $\ln k_{IAM}$ versus $1/T$ is called a van't Hoff plot. Its slope and intercept are $(-\Delta H^\circ/R)$ and $(\Delta S^\circ/R + \ln \Phi)$ respectively. The knowledge of V_{IAM} for the IAM column used [23] allows the determination of ΔS°.

2.3. Enthalpy–entropy compensation study

Linear relations between changes in enthalpy and entropy have been observed for a variety of processes [24]. This behaviour is labelled enthalpy–entropy compensation. The enthalpy–entropy compensation can be expressed by:

$$\Delta H^\circ = \beta \Delta S^\circ + \Delta G^\circ_\beta \quad (7)$$

where $\Delta G_\beta{}^\circ$ is the Gibbs free energy of a physico-chemical interaction at the compensation temperature β. According to Eq. (7), the slope of the enthalpy–entropy plot, β, is constant for processes exhibiting similar interaction mechanisms. When the enthalpy–entropy compensation is observed for a solute in a particular chemical interaction, the solute will have the same free energy ($\Delta G_\beta{}^\circ$) and the same net retention at the compensation temperature β, and is essentially retained by identical interaction mechanism, whatever the eluent composition.

2.4. Salt effects on probes retention

As previously described [20], the salt effect on the apparent equilibrium constant, K_{IAM}, can be described using a simplified model derived from the Wyman linkage relations. K_{IAM} for both specific and no specific interactions, and then k_{IAM}, can be linked to the changes in salt concentration, c, using the following equation:

$$\ln k_{IAM} = \ln k_0 + \Delta n \ln(1 + \kappa c) \quad (8)$$

Where Δn is the release parameter. It is related to the difference in the number of salt cations bound to the IAM/mobile phase interface before and after the interaction of the solute with the stationary phase. κ is the average additive binding constant of the salt and k_0 is the theoretical k-value for probe at $c = 0$. In this simplified model, the direct salt effect is the only one to be taken into account. The notion of change in the water activity and the existence of different sites of salt binding are not taken into account.

3. Experimental

3.1. Membrane probes selection

The probes studied were 1,6-diphenyl-1,3,5-hexatriene (DPH), 9-diethylamino-5H-benzo[α]phenoxazine-5-one or nile red (NR) and 2-(*p*-toluidinyl)naphtalene-6-sulfonate (TNS). Their molecular structures are presented in Fig. 2. TNS was an anionic probe whereas DPH and NR were neutral ones. They were formerly selected because of their fluorescent properties and use in lipid–calcium ion interaction studies by direct fluorescent measurements. NR is a polarity

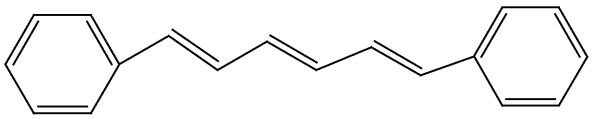

1,6-diphenyl-1,3,5-hexatriene (DPH)

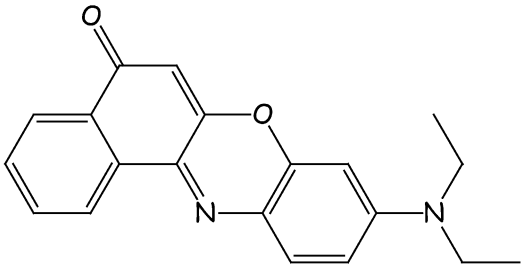

9-diethylamino-5H-benzo[α]phenoxazine-5-one

or nile red (NR)

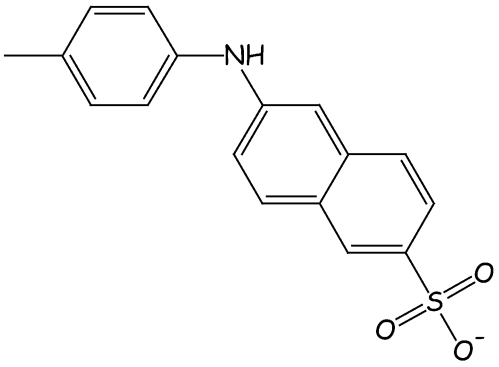

2-[p-toluidinyl]-naphtalene-6-sulfonate (TNS)

Fig. 2. Molecular structures of DPH, NR and TNS.

probe whose fluorescent properties strongly depend on the environment polarity [25]. NR was used to probe proteins or lipids [26,27]. DPH is known as a fluidity probe [28]. The fluidity of many lipid assemblies has been monitored with DPH [29,30]. TNS, as its parent compound 1-anilino-8-naphtalenesulfonate (ANS), are polarity and electric potential probes; they allow an estimate of electric potential at the surface of lipid vesicles [31] or of biological membranes [32,33].

3.2. Apparatus

Monitoring of chromatographic data was performed on a high-performance liquid chromatography (HPLC) system driven by the 32 Karat software version 5.0 from Beckman Coulter (Roissy, France). The system consisted of a 125 Beckman pump, a Rheodyne injection valve model 7725 (Cotati, USA) fitted with a 50 μL sample loop and a 168 Beckman diode-array detector. The detection wavelengths were set at 565, 355 and 320 nm for NR, DPH and TNS, respectively. The analytical columns were a (100 mm × 4.6 mm) IAM.PC.DD2 (Regis Technologies, Morton Grove, USA) with a particle size of 12 μm and a (150 mm × 4.6 mm) $5C_8$ Chromspher with a particle size of 8 μm. Both columns were supplied by Interchim (Montluçon, France). The columns were thermostated with a Croco-Cil temperature controller (±0.5 °C) provided by Interchim. Unless otherwise stated, experiments were performed at 25 °C. pH measurements were done with a Beckman 300 pH meter.

3.3. Reagents

All reagents were of analytical grade. 2-(*p*-Toluidinyl)naphtalene-6-sulfonic acid; potassium salt (TNS) was purchased from Sigma–Aldrich (Saint-Quentin Fallavier, France). 9-Diethylamino-5H-benzo[α]phenoxazine-5-one (NR), 1,6-diphenyl-1,3,5-hexatriene (DPH) and 1-(4-trimethylammoniumphenyl)-6-phenyl-1,3,5-hexatriene (TMA-DPH) were produced by Molecular Probes (Eugene, USA) and obtained from Interchim (Montluçon, France). All solvents were of analytical grade and spectroscopically tested before experiments. Acetonitrile was from Carlo Erba (Val de Reuil, France), sterile water for injection from Lavoisier (Paris, France), tetrahydrofuran from Prolabo (Fontenay-sous-bois, France). Imidazole was purchased from Sigma–Aldrich, chlorhydric acid from Labosi (Oulchy Le Château, France) and aqueous solutions of calcium chloride 10% (m/v) or sodium chloride 20% (m/v) from Aguettant (Lyon, France).

3.4. Operating methods

3.4.1. General procedures

The mobile phase consisted of a mixture of different proportions (v/v) of acetonitrile and 5 mM imidazole/HCl buffer adjusted to pH 7.1 and possibly spiked with calcium or sodium chloride. Unless otherwise stated, acetonitrile content in mobile phase was 50% (v/v) for NR and DPH; 20% (v/v) for TNS. The flow rate of the mobile phase was set in all cases at 1 mL min^{-1}.

10^{-3} M stock solutions of probes were prepared. TNS was dissolved in water whereas NR and DPH were both dissolved in tetrahydrofuran. All stock solutions were kept at +4 °C for 3 months. Stability of these solutions was checked by UV–vis measurements. TNS stock solution was daily diluted to 5×10^{-5} M in water before injection. NR and DPH stock solutions were first diluted to 10^{-4} M in acetonitrile, then to 10^{-5} M in acetonitrile–water (50:50 (v/v)) before injection. The injected volume was 50 μL in all cases. For each measurement, injections were performed in triplicate. V_{IAM}, the volume of stationary phase for the IAM.PC.DD2 column

used, equals 0.125 mL [23]. V_M, the volume of mobile phase, was measured by injecting a liquid mixture with a volume composition different from that of the mobile phase. It was equal to 1.45 mL.

3.4.2. Determination of the probes partition coefficients

The acetonitrile contents (v/v) in the mobile phase used to determine the partition coefficient of the probes were 40, 45, 50, 55 and 60% for DPH and NR; 10, 15, 20, 25 and 30% for TNS.

The calculated log *P* (C log *P*), theoretical *n*-octanol–water partition coefficients, were determined with the CS ChemDraw Ultra software from CambridgeSoft (Cambridge, USA).

3.4.3. Thermodynamic parameters of the probe-stationary phase interactions

Probes capacity factors were determined over the temperature range 25–45 °C. Experiments were performed at 25, 30, 35, 40 and 45 °C.

3.4.4. Calcium effect on the probes retention

Added calcium chloride concentrations in mobile phase were 2.5, 5, 10, 15 and 20 mM for DPH and NR; 1, 2, 4, 6, 10, 15 and 20 mM for TNS. The calcium concentrations included those frequently found in paediatric TPN mixtures, lying between 2.5 and 7.5 mM. For the enthalpy–entropy compensation study of TNS, the tested temperatures were 25, 30, 35, 40 and 45 °C for each calcium concentration.

The evolution of partition coefficients and thermodynamic parameters for the probes was investigated using the experimental conditions described in Sections 3.4.2 and 3.4.3 in the presence of 20 mM calcium chloride in the mobile phase, excepted for the TNS partition coefficient which was evaluated with solvent proportions equal to 15, 20, 25, 30 and 35% (v/v).

3.4.5. Sodium effect on TNS retention

The sodium chloride concentrations studied were 5, 10, 20, 40 and 60 mM. As for calcium, the sodium concentrations took into account values found in paediatric TPN mixtures, lying between 10 and 30 mM.

3.4.6. Statistical treatment

A least square regression (LSR) was used to verify the existence of linear relationship between ln k_{IAM} and the organic volume fraction (φ_{ACN}) or the inverse of the temperature ($1/T$). A one way analysis of variance was performed to check the significance of the slope. To assess if the intercept of LSR equation was or not significantly different from zero, a Student's *t*-test was carried out. The level of significance was always set at $p < 0.05$. Statistical treatment of data was done using Microsoft Excel software for the linear regression and Kaleidagraph (Synergy Software) for the non-linear regression. All results were expressed as mean ± standard deviation.

Table 1
Partition coefficient logarithm (log K_w) and calculated log *P* (*C* log *P*) for the probes

$[Ca^{2+}]$ (mM)	log K_W	C log *P*
DPH		
0	4.81 ± 0.05	5.64
20	4.76 ± 0.06	/
NR		
0	3.89 ± 0.04	4.62
20	3.80 ± 0.05	/
TNS		
0	3.03 ± 0.02	2.89
20	3.58 ± 0.04	/

See experimental conditions in Sections 3.4.2 and 3.4.4. /: not relevant.

4. Results and discussion

4.1. Determination of the probes partition coefficients

In order to determine their partition coefficients, the probes retention was studied in relation to the solvent proportion in the mobile phase. According to Eq. (2), linear plots were obtained between ln k_{IAM} and the acetonitrile volume fraction φ_{ACN} for the three probes in the absence or in the presence of calcium ions ($p < 0.05$). The correlation coefficients were at least equal to 0.996. The logarithms of extrapolated partition coefficient (log K_W) of each probe are presented in Table 1. In the absence of calcium chloride, DPH presented the greatest affinity to the phosphatidylcholine stationary phase, then NR and at last TNS. The log K_W values were in accordance with the C log *P* estimated for the probes. C log *P* calculations are recognised as a good estimation of the molecules lipophilicity. They usually are well correlated to analytes retention on the C_{18} or C_8 stationary phases [5]. Hence, our results suggested a probe retention mechanism on IAM stationary phase mostly ruled by hydrophobic forces. This partitioning mechanism implies that the solute molecule penetrates the head-group region of phosphatidylcholine and is embedded within the hydrocarbon region of the stationary phase [7]. Moreover, the existence of either repulsive or attractive electrostatic forces with the charged phosphate or ammonium groups of the IAM phase should be also taken into account for anionic TNS in addition with hydrophobic interactions; as suggested by its lower log K_W value (Table 1).

4.2. Thermodynamic parameters of the probe-stationary phase interactions

The dependence of the probes retention on temperature was studied in order to assess the thermodynamic parameters, in the absence and in the presence of calcium ions. van't Hoff plots, according to Eq. (6), are presented in Fig. 3 for DPH and NR. The van't Hoff plots for TNS in presence of various calcium concentrations are displayed in Fig. 4. In all cases, a linear fit was verified for the three probes with or without calcium addition to the mobile phase ($p < 0.05$). The

Table 2
Thermodynamic parameters ΔH°, ΔS°, $T\Delta S^\circ$ and ΔG° for DPH and NR from the mobile phase to the IAM stationary phase in relation to calcium concentration

[Ca^{2+}] (mM)	ΔH° (kJ mol^{-1})	ΔS° (J mol^{-1} K^{-1})	$T\Delta S^\circ$ (kJ mol^{-1})	ΔG° (kJ mol^{-1})
DPH				
0	−10.9 ± 0.2	−3.9 ± 0.1	−1.2 ± 0.1	−9.7 ± 0.2
20	−9.8 ± 0.2	−1.4 ± 0.1	−0.4 ± 0.0	−9.4 ± 0.2
NR				
0	−12.0 ± 0.2	−9.5 ± 0.2	−2.8 ± 0.0	−9.2 ± 0.2
20	−11.7 ± 0.2	−8.9 ± 0.2	−2.7 ± 0.0	−9.0 ± 0.3

See experimental conditions in Sections 3.4.3 and 3.4.4. Note that contribution of entropy to ΔG° is represented by $T\Delta S^\circ$, where T is 298 K (25 °C).

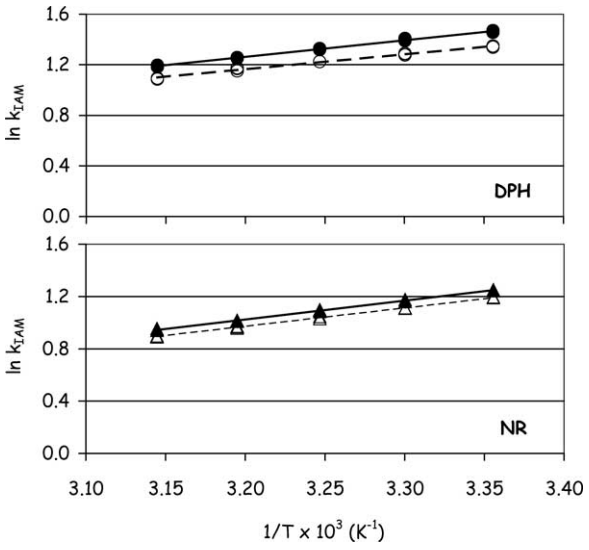

Fig. 3. Vant Hoff plots in the absence of calcium (closed symbols) and in the presence (open symbols) of 20 mM calcium for DPH (●,○) and NR (▲,△). For operating conditions: see Section 3.

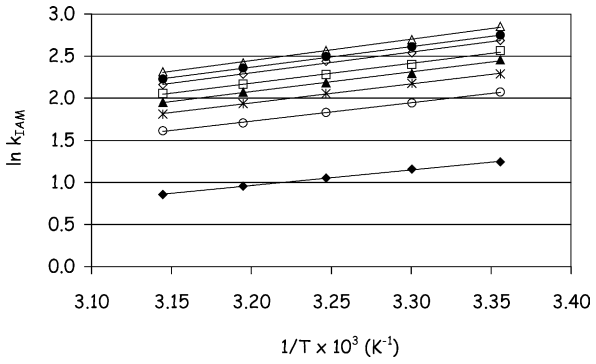

Fig. 4. TNS Vant Hoff plots for different mobile phase calcium concentrations. With [Ca^{2+}] = 0 (♦), 1 (◯), 2 (*), 4 (▲), 6 (□), 10 (◇), 15 (●), 20 (△) mM. For operating conditions: see Section 3.

correlation coefficients were in all cases superior to 0.996. Linear van't Hoff plots were in agreement with an unvaried retention mechanism for the probes in the temperature range tested.

The thermodynamic parameters obtained from van't Hoff plots are presented in Table 2 for DPH and NR. Their dependence upon various calcium concentrations is detailed in Table 3 for TNS.

The Gibbs free energy, ΔG°, of solute transfer from the mobile phase to the stationary phase was negative for all probes with or without calcium indicating that solute transfer is a spontaneous process. The experiments showed that the more negative the ΔG° value, the longer the retention time, so the more efficient the probe transfer from the mobile to the stationary phase, in accordance with Eq. (4).

For all probes, increasing the temperature caused a decrease in the capacity factors, leading to negative values for ΔH°. This behaviour is in agreement with the temperature dependence of the hydrophobic effects which drive the partitioning in many bilayer systems [34]. Negative ΔH° values indicated that the solute transfer is an exothermic process. Then, it is energetically more favourable for the probes to be in the stationary phase than in the mobile phase.

The observed negative ΔS° values proved the loss of the degree of freedom of the probes when included in the IAM phase. The latter is probably due to the involvement of interactions between the probes and the stationary phase. The probes could be embedded along the diacyl chains of the

Table 3
Thermodynamic parameters ΔH°, ΔS°, $T\Delta S^\circ$ and ΔG° for TNS from the mobile phase to the IAM stationary phase in relation to calcium concentration

[Ca^{2+}] (mM)	ΔH° (kJ mol^{-1})	ΔS° (J mol^{-1} K^{-1})	$T\Delta S^\circ$ (kJ mol^{-1})	ΔG° (kJ mol^{-1})
0	−15.6 ± 0.2	−21.6 ± 0.4	−6.4 ± 0.1	−9.2 ± 0.3
1	−18.2 ± 0.2	−23.5 ± 0.3	−7.0 ± 0.1	−11.2 ± 0.2
2	−18.9 ± 0.2	−23.9 ± 0.4	−7.1 ± 0.1	−11.8 ± 0.2
4	−19.4 ± 0.3	−24.5 ± 0.6	−7.3 ± 0.2	−12.1 ± 0.4
6	−19.7 ± 0.3	−24.6 ± 0.5	−7.3 ± 0.2	−12.4 ± 0.3
10	−20.4 ± 0.4	−25.8 ± 0.6	−7.7 ± 0.2	−12.7 ± 0.4
15	−20.4 ± 0.2	−25.3 ± 0.3	−7.6 ± 0.2	−12.9 ± 0.2
20	−21.2 ± 0.3	−27.1 ± 0.6	−8.1 ± 0.2	−13.1 ± 0.4

See experimental conditions in Sections 3.4.3 and 3.4.4. Note that contribution of entropy to ΔG° is represented by $T\Delta S^\circ$, where T is 298 K (25 °C).

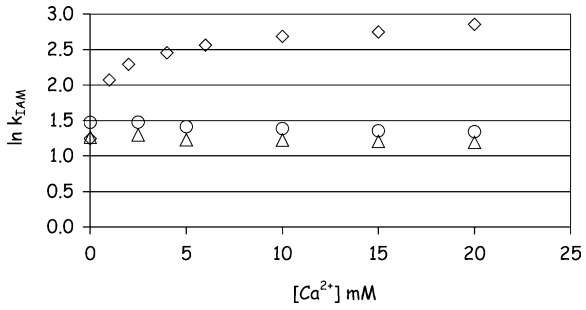

Fig. 5. Effect of mobile phase calcium concentration on the retention of DPH (◯), NR (△) and TNS (◊) at 25 °C. For operating conditions: see Section 3.

IAM support according the partitioning mechanism previously described, particularly DPH for which the tendency to predominantly orient parallel to the fatty acyl chains of the membrane bilayer is reported [35]. DPH, the most hydrophobic probe, is supposed to exclusively establish hydrophobic interactions with unsaturated long acyl chains of IAM. NR, because of its hetero-atomic structure, could involve hydrogen bonds with IAM whereas anionic TNS could be able to establish electrostatic forces with immobilised phosphatidylcholine.

When ΔH° was compared to $T\Delta S^\circ$ in Tables 2 and 3, the magnitude of ΔH° was always greater than the one of $T\Delta S^\circ$, over the temperature range studied. Hence, enthalpy plays a greater role in the retention process than entropy does. The solute transfer from the mobile to the stationary phase is consequently enthalpically driven (i.e. governed by hydrophobic effect), especially for DPH and NR. Indeed, for TNS the entropic contribution (related to steric hindrance) appears relatively greater than for the other probes, certainly due to the additive repulsive/electrostatic interactions with the polar head-groups of IAM.

4.3. The role of calcium ions on probe retention: assumptions

The role of calcium ions on probe retention is illustrated in Fig. 5. In relation to calcium concentrations, DPH and NR capacity factors only exhibited a slight decrease, whereas that of TNS increased [analysis of variance (ANOVA) test, $p < 0.05$)].

4.3.1. DPH and NR

The decrease of retention for DPH and NR may result from the calcium ions effect either on the mobile phase or on the stationary phase.

ΔS°, the standard entropy of transfer of the probes from the mobile phase to the stationary phase, increased for DPH and NR in the presence of calcium ions (Student's *t*-test, $p < 0.05$). Higher ΔS° values observed are related to a probe entropy increase in the IAM phase and/or a probe entropy decrease in the mobile phase.

The entropy increase in IAM phase reflects a less ordered environment of DPH and NR. Calcium ions, by interacting with the negative phosphate groups of the stationary phase, could form bridges between phosphate groups of two phosphatidylcholine molecules reducing both lipid motion freedom and water penetration [36]. This phenomenon could prevent DPH and NR from penetrating the interfacial region and then from being embedded within the hydrocarbon region.

The entropy decrease in mobile phase is in agreement with a more ordered environment of DPH and NR. The entropy decrease could result from the addition into the mobile phase of kosmotropic ions such as Ca^{2+}, known to bind adjacent water molecules more strongly than water molecules between themselves. Thus, the entropy of the system decreases due to increased water structuring around the ion [37,38].

In order to discriminate on which phase calcium effects are predominant, retention measurements were also performed on a C_8 stationary phase for DPH and NR in the same experimental conditions as on IAM chromatography. DPH and NR retention decreased with 20 mM $CaCl_2$ as shown by $\ln k$ values, which varied from 2.55 to 2.42 and from 1.40 to 1.30 for DPH and NR, respectively (data not shown). Hence, the common decrease in retention observed on either C_8 or IAM stationary phases is in accordance with a predominant calcium effect on mobile phase, without excluding a possible influence of calcium ions on IAM phase.

4.3.2. TNS

Concerning TNS (Table 3), in contrast to DPH and NR, the calcium ions made ΔG° becoming more negative (Student's *t*-test, $p < 0.05$) indicating a more efficient partitioning of TNS. ΔH° and ΔS° also became more negative in the presence of calcium (Student's *t*-test, $p < 0.05$). As the direct ion-pairing between calcium ions and TNS in the mobile phase seems highly unlikely, the TNS partition coefficient enhancement (Student's *t*-test, $p < 0.05$), shown in Table 1, could result from a direct interaction of Ca^{2+} ions with phosphate groups of phosphatidylcholine monolayer, leading to a positively charged stationary phase. Thus, anionic TNS would involve attractive electrostatic interactions, yielding to an increase of the retention.

Subsequently, it was assumed that there was a negative surface charge on the zwitterionic phosphatidylcholine membrane. Thus, we considered to determine the retention measurements of a cationic membrane probe with and without calcium in the mobile phase to verify this hypothesis. The probe 1-(4-trimethylammoniumphenyl)-6-phenyl-1,3,5-hexatriene, a cationic parent compound of DPH, was the most retained among all probes in the absence of $CaCl_2$ ($\ln k = 1.667$) and became the less retained in the presence of 20 mM $CaCl_2$ ($\ln k = 0.136$). These results confirmed the existence of a globally negative surface charge on the IAM phase, despite its zwitterionic chemical structure, exerting repulsive electrostatic forces towards TNS in the absence of cations. This observation could be related to the presence of

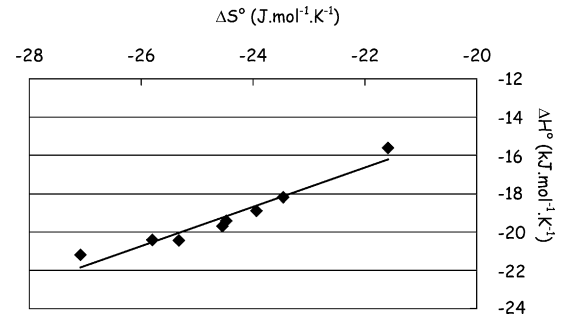

Fig. 6. Enthalpy–entropy compensation plot $\Delta H^\circ = f(\Delta S^\circ)$ for TNS at the different mobile phase calcium concentrations. For operating conditions: see Section 3.

negatively charged silanol groups (pK_a 6.8 ± 0.2 [39]) on the IAM.PC.DD2 support, as previously described [23,40–42].

4.4. Enthalpy–entropy compensation study for TNS retention in relation to calcium concentration

As TNS showed a dramatic retention increase upon calcium addition, in contrast to DPH and NR, an enthalpy–entropy compensation study in relation to calcium concentrations was performed for this probe in order to get a better insight into the interaction mechanisms involved. According to Eq. (7), ΔH° as a function of ΔS° determined at the different values of calcium concentration was plotted (Fig. 6). The corresponding LSR equation was characterised by a slope and an intercept different from zero and a correlation coefficient equal to 0.969, thus indicating that the enthalpy–entropy compensation was verified. The compensation temperature β was equal to 1026 K. This value is greater than previous compensation temperatures calculated for other hydrophilic/hydrophobic chromatographic systems [19,21]. This may be related to a difference in stationary phase bonding density which contributes very significantly to the β value [43]. Enthalpy–entropy compensation showed that TNS–IAM interaction mechanisms are independent of the calcium concentration values. That means, first, that TNS binds to the same location on IAM.PC.DD2 support whatever the calcium concentration and, second, that the possible interaction of Ca^{2+} with TNS binding site on IAM support is probably negligible. Assuming that Ca^{2+} cation and TNS preferentially interact with negative phosphate groups and with positive ammonium groups of IAM phase respectively (see Fig. 1), then the probable interaction of Ca^{2+} with phosphate groups will not alter the TNS–ammonium groups interaction.

4.5. Calcium and sodium effects on TNS retention

In order to get a better insight into the interaction mechanisms between calcium ions and phosphatidylcholine, a study of the calcium and sodium effects on TNS retention has been carried out. As shown in Fig. 7, the retention of TNS

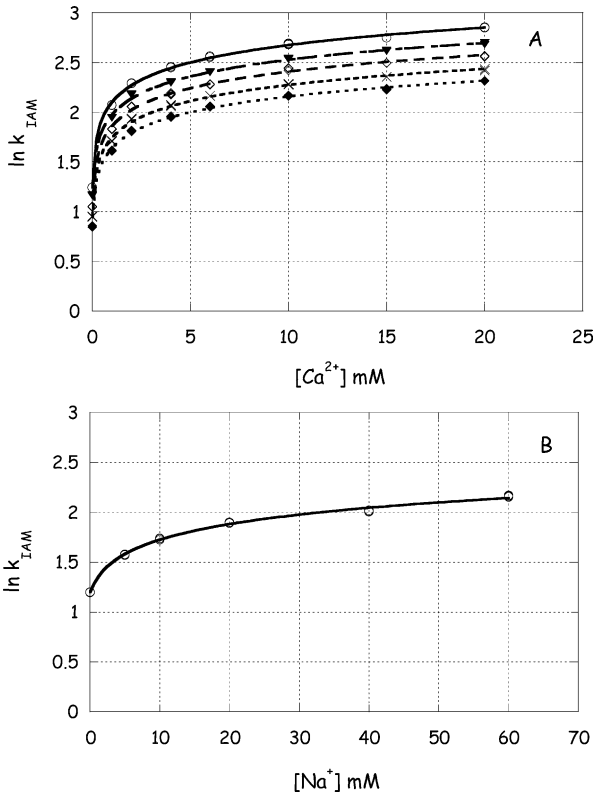

Fig. 7. Plots of ln k_{IAM} recreated from Eq. (8) for TNS versus [$CaCl_2$]: (A) at 25 °C (◯), 30 °C (▼), 35 °C (◊), 40 °C (×), 45 °C (♦) and versus [NaCl]: (B) at 25 °C. For operating conditions: Section 3.

increased according to logarithmic curves with the addition of calcium chloride (Fig. 7A) and sodium chloride (Fig. 7B) as well. For similar ionic strength, calcium increased TNS retention more than sodium, indicating that the affinity of Ca^{2+} to stationary phase appeared superior to that of Na^+. This feature was well correlated with the classification following the Hofmeister series established for both cations and anions. These series reflect the order of increasing polarisability and the ability for cations and anions to interact with negative and positive groups respectively [44]. For instance, cations and anions can be classified as follows: $K+ \approx \mathbf{Na^+} < NH^{4+} < Li^+ < Tl^+ < Ag^+ < Ba^{2+} \approx Sr^{2+} < Co^{2+} < \mathbf{Ca^{2+}} < Cu^{2+} < Cd^{2+} < Zn^{2+} < Ce^{3+}$ and $SO_4{}^{2-} < \mathbf{Cl^-} < NO_2{}^- < CNO^- < Br^- < NO_3{}^- < ClO_3{}^- < I^- < ClO_4{}^-$ [44,45]. IAM stationary phase involves positively (ammonium) and negatively (phosphate) charged functionalities in close proximity to each other (Fig. 1). In the presence of $CaCl_2$ into the mobile phase, two interactions could occur: a weak one between Cl^- and the outer ammonium group and a strong one between Ca^{2+} and the inner phosphate group probably, as predicted by the Hofmeister series. These interactions between zwitterionic stationary phase and mobile phase cations and anions lead to the establishment of an ionic double layer. TNS retention on IAM is ruled by its ability to penetrate the electrostatic field established by the stationary phase. In the absence of cations, the negative

Table 4
Parameters $\ln k_0$, Δn and κ for sodium chloride (Na^+) and calcium chloride (Ca^{2+}), calculated by fitting the curves $\ln k_{IAM} = f([\text{cation}])$ with Eq. (8)

Temperature (°C)	$\ln k_0$	Δn	κ (M^{-1})	r^*
Na^+				
25	1.20 ± 0.01	0.25 ± 0.01	0.74 ± 0.09	0.998
Ca^{2+}				
25	1.24 ± 0.01	0.25 ± 0.00	28.20 ± 2.81	0.999
30	1.16 ± 0.01	0.24 ± 0.01	26.92 ± 3.02	0.999
35	1.05 ± 0.01	0.24 ± 0.01	27.21 ± 3.21	0.999
40	0.95 ± 0.01	0.23 ± 0.01	28.59 ± 3.43	0.999
45	0.85 ± 0.01	0.23 ± 0.00	29.80 ± 2.82	0.999

See experimental conditions in Sections 3.4.4 and 3.4.5.
* Correlation coefficient for non-linear regression.

surface charge exerts a repelling effect on TNS. With $CaCl_2$ IAM phase was positively charged, allowing TNS to greatly interact with the stationary phase. With NaCl, the effect was weaker than with $CaCl_2$, as previously described. In order to quantify this feature, κ the average additive binding constants of cations were calculated. The Wyman simplified model (Eq. (8)) was used to fit the experimental curves shown on Fig. 7. Δn, the release parameter, and k_0, the theoretical k-value for TNS at a salt concentration equal to zero, were also calculated. Data are presented in Table 4. The correlation coefficients were at least equal to 0.999 meaning that the simplified Wyman model seems to be appropriate to fit our data. This simplified model only took into account the direct salt effect, involving identical and independent sites for salt binding. Thus, and as already stated, the change in water activity or the existence of different salt binding sites are probably negligible in our case. As expected, the binding constant of Ca^{2+} for IAM was much higher than Na^+ binding constant ($p < 0.05$) and appeared independent of temperature. Positive Δn values are in accordance with a salt fixation on IAM; TNS interaction with IAM stationary phase leads to the neutralisation of a positive charge, thus making easier calcium or sodium adsorption. The very similar Δn values for Na^+ and Ca^{2+} suggest that the number and the nature of binding sites are identical for both salts.

As IAM phase is demonstrated to interact with cations, lipid emulsions in TPN mixtures are also known to strongly interact with cations [46]. The stability of lipid emulsions has been explained by the DLVO (Derjaguin, Landau, Verwey, Overbeek) theory of colloid stability [47]. The cations interact with charged colloids, and with lipid droplets as well, by two mechanisms: non-specific and specific adsorption [1]. Non-specific adsorption occurs when ions are only bound to lipid droplets by electrostatic forces. This behaviour is typical of monovalent cations such as Na^+ on phospholipid surfaces [48]. The surface charge of lipid droplets, negative in the absence of ions, will increase with sodium addition until zero at high salts concentrations. Since the only force causing adsorption is electrostatic, no further ion adsorption can occur when the surface charge is nil. By contrast, specific adsorption occurs when an ion interacts with the surface chemically as well as electrostically. This behaviour is typical of Ca^{2+} cations known to be complexed by the lipid phosphate headgroups [48]. In the case of specific adsorption, many more ions can adsorb to the surface than is simply required to neutralize the droplet surface charge. Then the lipid surface charge, negative in the absence of ions, will acquire a positive charge due to calcium ions adsorption. This process is called charge reversal and is characteristic of the specific adsorption phenomenon. These mechanisms described for cations in TPN mixtures are in accordance with our chromatographic data.

5. Conclusion

The present work showed that IAM chromatography is an adequate method to determine the partition coefficients of membrane probes. Partition coefficients of the probes obtained with IAM chromatography confirmed their affinity for the lipid phase of the emulsion as qualitatively assumed from direct fluorescence measurements. Thanks to the versatility of chromatography, the measurement of thermodynamic parameters of the probes partitioning was possible with convenient precision. The existence of a spontaneous negative charge on the IAM surface, despite the zwitterionic character of phosphatidylcholine, was also shown by the higher affinity of TMADPH for IAM phase, compared to that of DPH. This feature underlines the similarity between IAM stationary phase and natural phospholipids of lipid emulsion. This negative charge can be related to the presence of negatively charged silanol groups on the IAM.PC.DD2 support, but it can be reasonable to assume that secondary effects of free silanols on analyte retention are probably negligible compared to specific effects of phosphatidylcholine grafted molecules. However, in order to study an even more realistic model of lipid emulsion, the perfusion on a reversed-phase column of an egg-phospholipids solution [49], whose composition is identical to lipid emulsion phospholipids, should be considered in the future.

IAM chromatography was also demonstrated convenient for studying calcium and sodium effects. Ion effects were quantified in terms of Wyman parameters, allowing the binding constants of calcium and sodium on the spontaneously charged IAM surface to be determined. Lastly, it was shown that chromatographic experiments were in accordance with previous works describing the interactions between electrolytes and lipid emulsion in TPN mixtures [1].

Eventually, IAM chromatography confirmed spectrofluorometric measurements and moreover refined the determination of quantitative data. Consequently, IAM chromatography certainly appears as a suitable mimetic system for studying interactions in TPN mixtures and particularly to study cations interactions with phospholipids.

Acknowledgements

We would like to thank Dr. A. Kasselouri for helpful discussion. V. Hernando acknowledges with gratitude financial support (AHR 2003) from Assistance Publique-Hôpitaux de Paris (AP-HP) and CNRS (Centre National pour la Recherche Scientifique).

References

[1] C. Washington, Int. J. Pharm. 66 (1990) 1.
[2] V. Hernando, A. Rieutord, F. Brion, P. Prognon, Talanta 60 (2003) 543.
[3] J. Férézou, N. Lai, C. Leray, T. Hajri, A. Frey, Y. Cabaret, J. Courtieu, C. Lutton, A. Bach, Biochim. Biophys. Acta 1213 (1994) 149.
[4] G. Chansiri, R. Lyons, M. Patel, S. Hem, J. Pharm. Sci. 88 (1999) 454.
[5] T. Geetha, S. Singh, PSTT 3 (2000) 406.
[6] C. Lepont, C. Poole, J. Chromatogr. A 946 (2002) 107.
[7] S. Ong, H. Liu, C. Pidgeon, J. Chromatogr. A 728 (1996) 113.
[8] G. Caldwell, J. Masucci, M. Evangelisto, R. White, J. Chromatogr. A 800 (1998) 161.
[9] S. Ong, H. Liu, X. Qiu, G. Bhat, C. Pidgeon, Anal. Chem. 67 (1995) 755.
[10] X.-Y. Liu, Q. Yang, M. Hara, C. Nakamura, J. Miyake, Mater. Sci. Eng. C 17 (2001) 119.
[11] M. Abraham, H. Chadha, R. Leitao, R. Mitchell, W. Lambert, R. Kaliszan, A. Nasal, P. Haber, J. Chromatogr. A 766 (1997) 35.
[12] F. Barbato, M. La-Rotonda, F. Quaglia, Eur. J. Med. Chem. 31 (1996) 311.
[13] L. Escuder-Gilabert, S. Sagrado, R. Villanueva-Camanas, M. Medina-Hernandez, J. Chromatogr. B 740 (2000) 59.
[14] F. Barbato, B. Cappello, A. Miro, M. La-Rotonda, F. Quaglia, Farmaco 53 (1998) 655.
[15] A. Nasal, M. Sznitowska, A. Bucinski, R. Kaliszan, J. Chromatogr. A 692 (1995) 83.
[16] H. Mozsolits, T. Lee, H. Wirth, P. Perlmutter, M. Aguilar, Biophys. J. 77 (1999) 1428.
[17] W. Hu, P. Haddad, K. Hasebe, M. Mori, K. Tanaka, M. Ohno, N. Kamo, Biophys. J. 83 (2002) 3351.
[18] D. Cohen, M. Leonard, J. Lipid Res. 36 (1995) 2251.
[19] M. Haroun, C. Dufresne, E. Jourdan, A. Ravel, C. Grosset, A. Villet, E. Peyrin, J. Chromatogr. A 977 (2002) 185.
[20] I. Slama, C. Ravelet, C. Grosset, A. Ravel, A. Villet, E. Nicolle, E. Peyrin, Anal. Chem. 74 (2002) 282.
[21] W. Melander, D. Campbell, C. Horvath, J. Chromatogr. 158 (1978) 215.
[22] D. Reymond, G. Nghi-Chung, J. Mayer, B. Testa, J. Chromatogr. 391 (1987) 97.
[23] A. Taillardat-Bertschinger, A. Galland, P.-A. Carrupt, B. Testa, J. Chromatogr. A 953 (2002) 39.
[24] L. Sander, L. Field, Anal. Chem. 52 (1980) 2009.
[25] J. Deye, T. Berger, Anal. Chem. 62 (1990) 615.
[26] P. Greenspan, S. Fowler, J. Lipid Res. 26 (1985) 781.
[27] D. Sackett, J. Wolff, Anal. Biochem. 167 (1987) 228.
[28] B. Lentz, Chem. Phys. Lipids 50 (1989) 171.
[29] V. Ben-Yashar, Y. Barenholz, Chem. Phys. Lipids 60 (1991) 1.
[30] B. Lentz, Chem. Phys. Lipids 64 (1993) 99.
[31] M. Eisenberg, T. Gresalfi, T. Riccio, S. McLaughlin, Biochemistry 18 (1979) 5213.
[32] M. Sugawara, M. Kurosawa, K. Sakai, M. Kobayashi, K. Iseki, K. Miyazaki, Biochim. Biophys. Acta 1564 (2002) 149.
[33] M. Komorowska, A. Czarnoleski, Colloid Surf. B 20 (2001) 309.
[34] W. Wimley, S. White, Biochemistry 32 (1993) 6307.
[35] R. Kaiser, E. London, Biochemistry 37 (1998) 8180.
[36] D. Zubiri, A. Domecq, D. Bernik, Colloid Surf. B 13 (1999) 13.
[37] B. Hribar, N. Southall, V. Vlachy, K. Dill, J. Am. Chem. Soc. 124 (2002) 12302.
[38] J. Grigsby, H. Blanch, J. Prausnitz, Biophys. Chem. 91 (2001) 231.
[39] P. Schindler, H. Kamber, Helv. Chim. Acta 51 (1968) 1781.
[40] C. Ottiger, H. Wunderli-Allenspach, Pharm. Res. 16 (1999) 643.
[41] A. Mälkiä, L. Murtomäki, A. Urtti, K. Kontturi, Eur. J. Pharm. Sci. 23 (2004) 13.
[42] M. Amato, F. Barbato, P. Morrica, F. Quaglia, M. La-Rotonda, Helv. Chim. Acta 83 (2000) 2836.
[43] L. Cole, J. Dorsey, Anal. Chem. 64 (1992) 1317.
[44] H. Cook, G. Dicinoski, P. Haddad, J. Chromatogr. A 997 (2003) 13.
[45] H. Cook, W. Hu, J. Fritz, P. Haddad, Anal. Chem. 73 (2001) 3022.
[46] W. Dawes, M. Groves, Int. J. Pharm. 1 (1978) 141.
[47] M. Barnett, Nutrition 5 (1989) 348.
[48] C. Washington, Adv. Drug Deliv. Rev. 20 (1996) 131.
[49] W. Hu, P. Haddad, K. Tanaka, M. Mori, K. Tekura, K. Hasebe, M. Ohno, N. Kamo, J. Chromatogr. A 997 (2003) 237.